

STUDY ON SPATIAL CORRELATION STRUCTURE OF FLUCTUATING PRESSURE ACTING ON A CIRCULAR CYLINDER

Minoru Noda⁺¹, Shinya Onishi⁺² and Fumiaki Nagao⁺³

⁺¹Tokushima University, Tokushima, Japan

⁺²Graduate school of Tokushima University, Tokushima, Japan

⁺³Tokushima University, Tokushima, Japan

In this study, the spatial correlation structure of fluctuating surface pressure acting on a fixed circular cylinder was investigated by wind tunnel tests and the computational fluid dynamics (CFD). Our study involved an examination of the following two effects: 1.) the aspect ratio of the model and 2.) the boundary conditions of the sidewalls for CFD on the fluctuating surface pressure acting on a fixed circular. This study produced the finding that the special correlation of the fluctuating pressure on a fixed circular cylinder was affected by the aspect ratio of the model. A proper orthogonal decomposition (POD) analysis indicated that the fluctuating surface pressure acting on a circular cylinder had symmetric and asymmetric mode shapes along the axis of the cylinder, and these modes affected the spatial correlation of the fluctuating aerodynamic forces acting on the cylinder.

Keyword: Coherence, Aspect ratio, Boundary condition, Proper orthogonal decomposition (POD) analysis

1. INTRODUCTION

A circular cylinder is a fundamental element of structures such as the cables of cable-stayed bridges, and transmission lines. However, since the stiffness and damping of these members are low, they often show aerodynamic instability in wind. One of the causes of aerodynamic instabilities is the periodic pressure fluctuation acting on the surface of these members caused by Karman's vortex. If the member is short, the fluctuating surface pressure due to Karman's vortex has complete correlation along the axis of the cylinder. However, in the case of long members, the fluctuating surface pressure acting on the cylinder shows complex behavior, and the spatial correlation along the cylinder axis is reduced. Therefore, it is necessary to understand the spatial correlation characteristics of fluctuating pressure when the member is long in order to accurately estimate the aerodynamic response of those members, and many researchers have investigated this phenomenon for rectangular cylinders. Vickery investigated the spatial correlation of fluctuating lift and drag acting on a square prism in smooth and turbulent flows¹⁾. On the other hand, the spatial correlation of fluctuating velocity near a circular cylinder was investigated by El Baroudi²⁾. In this study, the correlation coefficient of fluctuating velocity between two points near a circular cylinder was measured and it was found that the correlation length became about three to six times the diameter of the circular cylinder. Moreover, the correlation coefficient of fluctuating forces on a circular cylinder was measured by Keefe³⁾. This investigation indicated that the correlation length of fluctuating forces was about five times the diameter of the circular cylinder. However, the correlation structure of fluctuating surface pressure on a circular cylinder has not yet been clarified in detail.

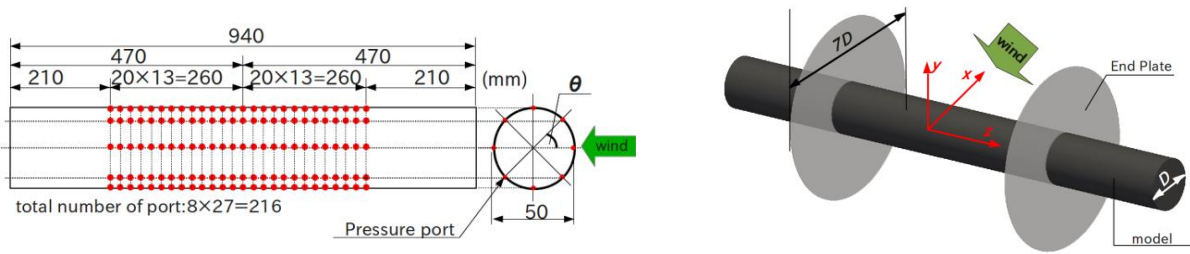
In addition, it is important to maintain reproducibility in terms of the fluctuation of aerodynamic forces on cylindrical models in wind tunnel tests. However, it is not clear at which level the aspect ratio of cylindrical models should be maintained in order to reproduce the fluctuation aerodynamic forces on slender models. Therefore, the effects of the aspect ratio of the circular cylinder for wind tunnel tests on fluctuating aerodynamic forces acting on a circular cylinder have not been investigated yet. Furthermore, the effects of the boundary condition of sidewalls on the numerical field for computational fluid dynamics (CFD) should also be clarified.

⁺¹noda@ce.tokushima-u.ac.jp, ⁺²c501431027@tokushima-u.ac.jp, ⁺³fumi@ce.tokushima-u.ac.jp

In this study, the spatial correlation structure of fluctuating surface pressure acting on a fixed circular cylinder was investigated by proper orthogonal decomposition (POD) analysis for wind tunnel tests and computational fluid dynamics (CFD) with large eddy simulation (LES).

2. CONFIGURATION OF WIND TUNNEL TEST

Fig. 1 shows the configuration of the wind tunnel tests. The circular cylinder model shown in Fig. 1 (a) was used. The diameter of the circular cylinder, D , was 50 mm, and the length of the model, L , was 940 mm. Therefore, the maximum aspect ratio, L/D , was 18.8. This model had 27 cross sections with 8 pressure holes arranged at equal intervals in the circumferential direction as shown in Fig. 1 (a). This model was placed at the center of the test section whose width, height, and length were 1,000, 1,500, and 4,000 mm, respectively. The aspect ratio was changed in the range from 3.6 to 10.8 by installing end plates whose diameter and thickness were 350 ($7D$) and 1.5 mm, respectively, as shown in Fig. 1 (b). In this study, the wind speed, U , was changed in the range from 4 to 10 m/s. This wind speed range corresponds to the range of Reynolds numbers from 13,000 to 33,000. The pressure at all the pressure holes was simultaneously measured at a 1 kHz sampling rate for a period of 40 s.



(a) Arrangement of pressure ports on the model (b) End plates on the model to change the aspect ratio

Figure 1. Experimental configuration.

3. CONFIGURATION OF CFD

Fig. 2 shows the numerical grid for LES. In this study, an LES of which the sub-grid scale model was a standard Smagorinsky model, was carried out by OpenFOAM⁴⁾ based on the finite volume method (FVM). The width of the numerical region was changed in the range from $2.7D$ to $10D$ to investigate the effects of aspect ratio on the aerodynamic forces. The number of grids was specified as shown in Tab. 1. The boundary conditions of the sidewalls were cyclic and slip. In this calculation, the Reynolds number, Re , was set to 20,000. The pressures at the points on the surface in the 40 s during which the flow became a stationary state were recorded at a 100 Hz sampling rate.

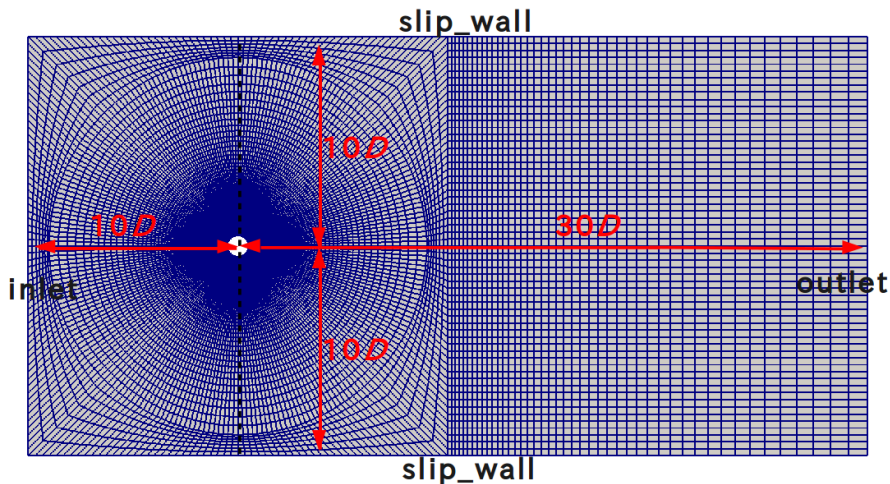


Figure 2: Numerical grid for LES.

Table 1: Number of grids along circumferential and axial directions.

| Case | Circumferential direction | Axial direction (Δz) |
|-------------------|---------------------------|--------------------------------|
| 2.7D-cyclic, slip | 240 | 90 (0.03D) |
| 5D-cyclic, slip | 240 | 60 (0.083D) |
| 10D-cyclic, slip | 240 | 120 (0.083D) |

4. RESULTS AND DISCUSSIONS

(1) Aerodynamic force coefficients

The obtained aerodynamic force coefficients acting on the whole circular cylinder are listed in Tab. 2. The CFD results for the different cases almost had the same value for the mean drag coefficient, C_D . The fluctuating drag and lift coefficients, $C_{D'}$ and $C_{L'}$, for the cyclic condition were higher than those for the slip condition. $C_{D'}$ and $C_{L'}$ for the cyclic condition decreased in proportion with the aspect ratio, L/D . Considering that strong fluctuating forces are produced by two-dimensional (2D) flows, it is found that the cyclic condition strengthens and the aspect ratio weakens the 2D structure of the flow. On the other hand, the C_D that was measured experimentally was higher than that obtained for CFD, and $C_{D'}$ and $C_{L'}$ were located between the slip and cyclic conditions. The reason for this is not clear.

Fig. 3 shows the power spectrum density (PSD) of the fluctuating lift for all cases. It is found that the Strouhal number stabilizes at 0.2 for all cases.

Table 2: Aerodynamic force coefficients.

| Case | C_D | $C_{D'}$ | $C_{L'}$ |
|----------------------|-------|----------|----------|
| 2.7D-cyclic | 1.161 | 0.115 | 0.303 |
| 2.7D-slip | 1.046 | 0.040 | 0.101 |
| 5D-cyclic | 1.167 | 0.084 | 0.270 |
| 5D-slip | 1.220 | 0.055 | 0.182 |
| 10D-cyclic | 1.174 | 0.053 | 0.256 |
| 10D-slip | 1.119 | 0.059 | 0.167 |
| Exp. ($Re=33,000$) | 1.321 | 0.079 | 0.217 |

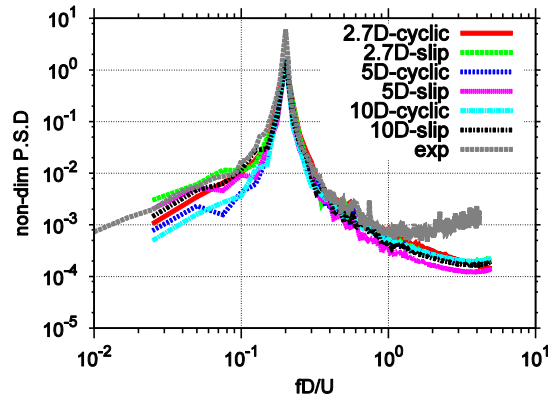


Figure 3: Power spectrum density of lift force.

(2) Spatial correlation of lift force

The root coherence of the fluctuating lift calculated between the middle of the span and each z/D is shown in Fig. 4. The curve in this figure is the Gaussian function defined by Eq. 1.

$$Rcoh = \exp\left\{-\frac{\pi}{4}\left(\frac{z}{L_c}\right)^2\right\} \quad (1)$$

where L_c is the correlation length based on the root coherence. Fitting formula (1) to the distribution of the root coherence for each case shown in Fig. 5 (a), the relation between the L_c and the L/D was obtained as shown in Fig. 5 (b). This figure shows that the correlation length for the cyclic condition is higher than that for the slip condition. Moreover, L_c decreases in proportion to L/D . This result reflects the results obtained for CFD in the previous section. On the other hand, L_c for CFD is higher than that measured experimentally at

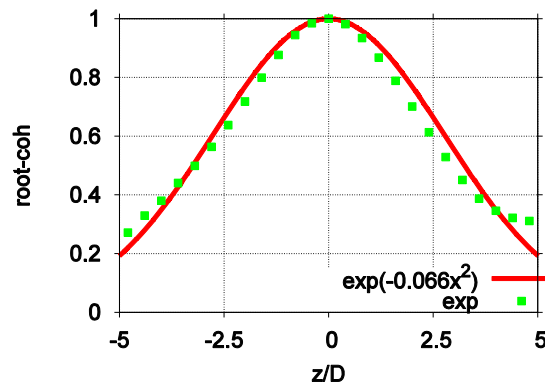
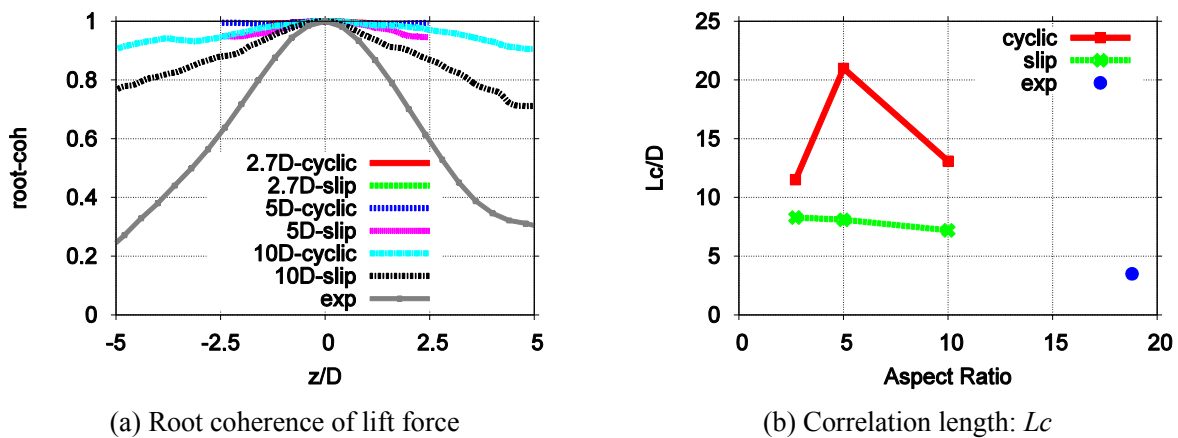


Figure 4: Root coherence distribution of lift force and fitting curve



(a) Root coherence of lift force

(b) Correlation length: L_c

$L/D=18.8$. Thus, it can be assumed that the L/D for this experiment was larger than for CFD.

(3) Structure of fluctuating surface pressure

The mechanism of the effects of the aspect ratio and the boundary condition of sidewalls on the special correlation of fluctuating aerodynamic forces on the circular cylinder was investigated by carrying out a proper orthogonal decomposition (POD) analysis⁵⁾ for the fluctuating surface pressure on the circular cylinder. Figs. 6 and 7 show the results of the POD analysis for the cases of the 2.7D-cyclic and the 10D-slip. In these figures, the longitudinal and transverse axes are defined as the angle of circumferential direction and the coordinate along the axial direction of the circular cylinder, respectively, as shown in Fig. 1. The pressure fluctuations from the 1st to the 5th mode are indicated as (a) – (e) in Figs. 6 and 7, and the power spectrum densities of the normal coordinate for each mode are shown as (f).

Figs. 6 and 7 indicate that the shapes of the 1st and 2nd modes were the same in both cases, and both modes were uniform along the axis of the cylinder. The power spectrum densities for the 1st and 2nd modes indicate that these two modes produce the fluctuating lift and fluctuating drag respectively, because the peak frequencies of these two modes were found to be equal to the Strouhal number and twice the Strouhal number, respectively. However, it is clear that the shapes of the mode were different between the cyclic condition and the slip condition in the case of the 3rd mode. The power spectrum densities of the 3rd, 4th, and 5th modes in the case of the 2.7D-cyclic indicate that these modes are independent of the fluctuations caused by the Karman vortex in Fig. 6. On the other hand, Fig. 7 shows that the 3rd and 5th modes, whose peak frequencies of the normal coordinates were equal to the Strouhal number, produced the fluctuating lift, whereas the 4th mode, whose peak frequency was determined to be twice the Strouhal number, produced the fluctuating drag.

The results for the modes beyond the 3rd mode for the other conditions are shown in Fig. 8. Figs. 6, 7, and 8 indicate that the modes representing the cyclic condition never showed an asymmetric pressure distribution responsible for producing the lift force. On the other hand, it is found that the modes for the slip

condition showed an asymmetric pressure distribution which could produce the lift force. Therefore, it can be said that the boundary condition of the sidewalls for CFD controls the mode shapes of higher degrees.

The modes and the power spectrum densities of each mode measured by using the wind tunnel test are presented in Fig. 9. This figure shows that the shapes of the modes for the result of the wind tunnel measurement were similar to the results obtained for the slip condition for CFD. In addition, it was found that the number of nodes along the axis of the cylinder increased in proportion with the mode degree as the common characteristics for the cases of the slip condition and the experiment.

The results of the POD analysis of the fluctuating surface pressure clarified that the cyclic condition of the sidewalls for CFD produced unnatural surface pressure fluctuation, and the slip condition of the sidewalls for CFD produced a similar pressure fluctuation in comparison with the experimental result. As the cause of this result, it can be mentioned that the flow fields near the sidewalls were forced to be the same by

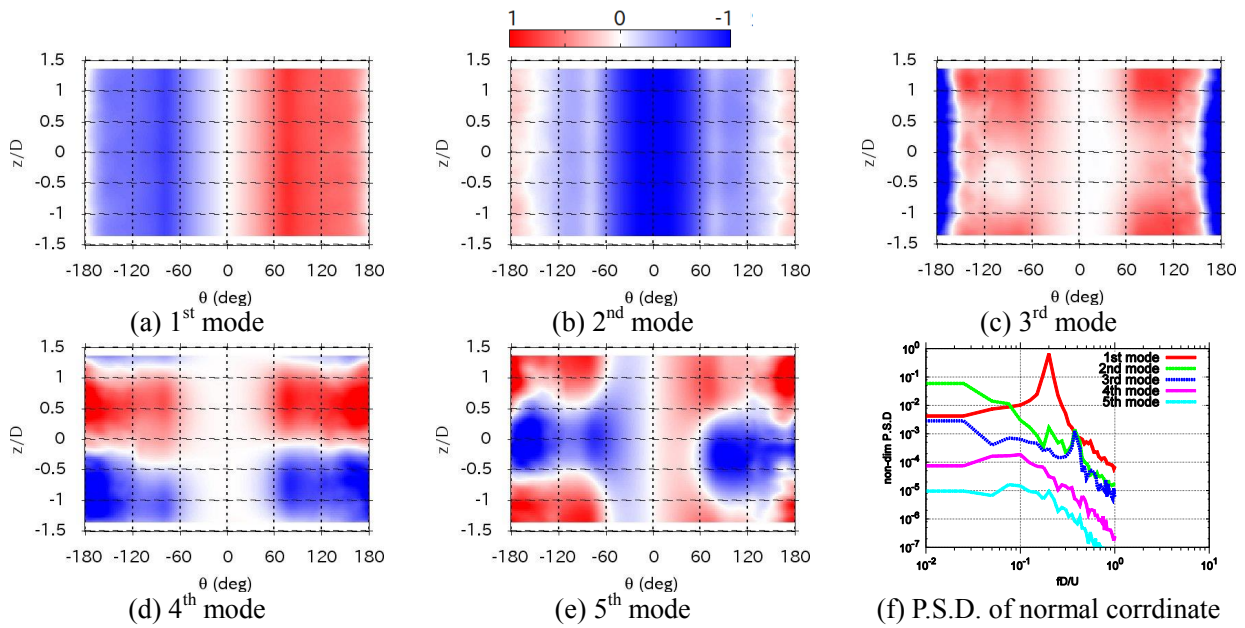


Figure 6: Result of POD analysis for CFD (2.7D-cyclic)

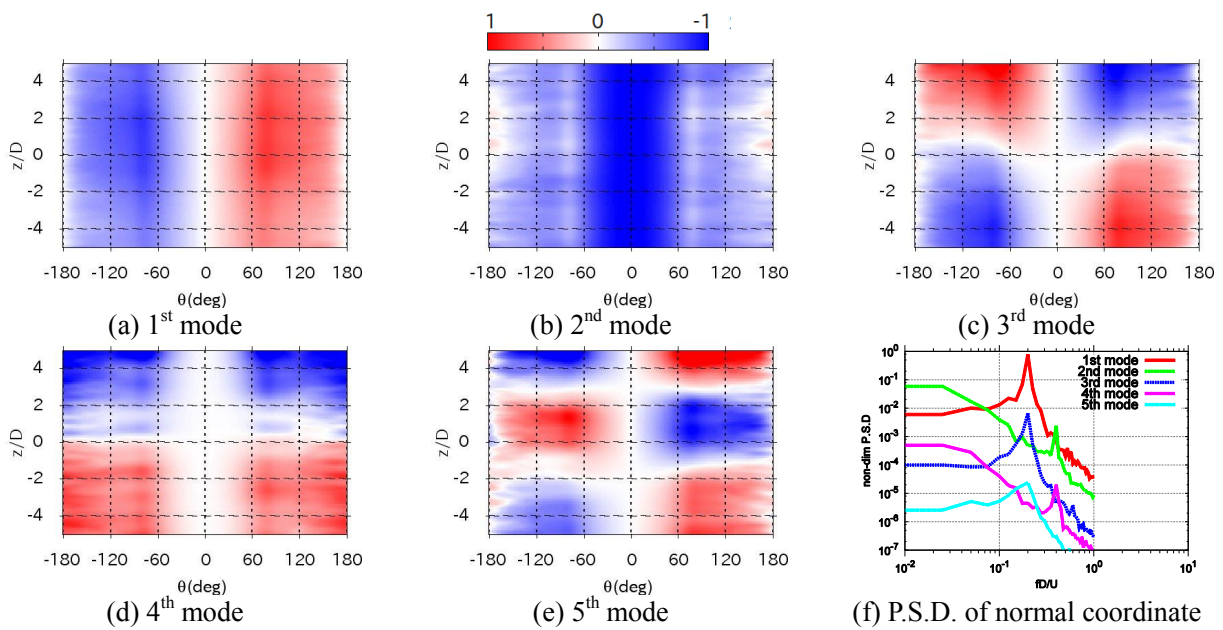


Figure 7: Result of POD analysis for CFD (10D-slip)

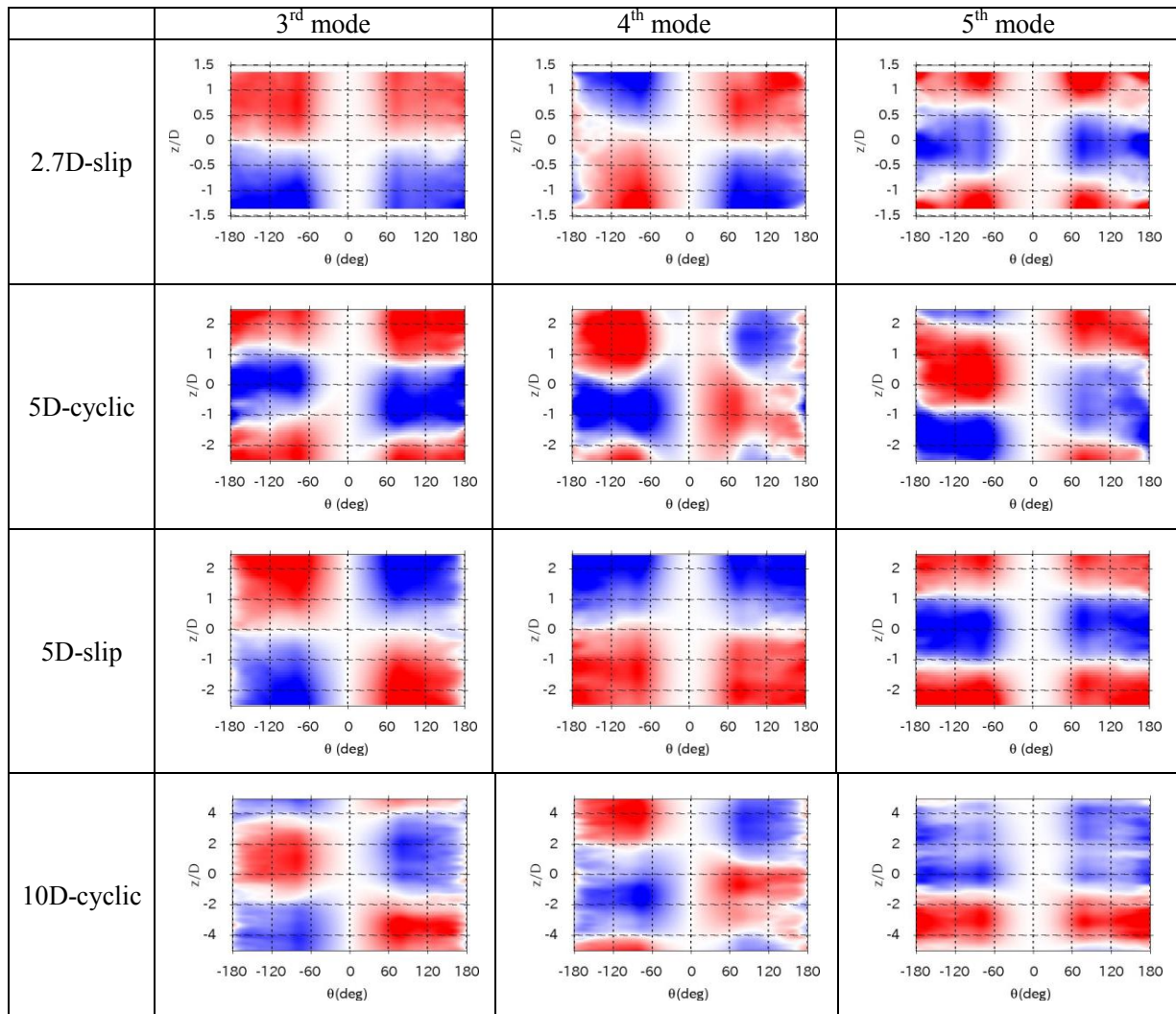


Figure 8: Results of POD analysis for each case

the cyclic condition. Therefore, the cyclic condition of sidewalls should not be used for the investigation of the correlation along the direction of the axis of the cylinder.

Fig. 10 indicates the contribution ratio for the results of the POD analyses. Fig. 10 (a) and (b) show the cumulative contribution ratio for all cases and the contribution ratio of the lift force component for the 2.7D-cyclic and experiment, respectively. Fig. 10 (a) shows that the cumulative contribution ratio up to the 2nd mode for the cyclic condition became large in comparison with the other cases. This result indicates that the 2D nature of the flow was strengthened because the cyclic condition of the 1st and 2nd modes, whose shapes were uniform along the cylinder axis, was strongly two-dimensional in nature. On the other hand, Fig. 10 (b) indicates that the fluctuating lift force depended on the 1st and 2nd mode shapes. Therefore, the spatial correlation along the axis of the cylinder is strengthened by the 1st and 2nd mode and weakened by modes larger than the 3rd degree.

5. CONCLUSION

In this study, the fluctuating forces acting on a fixed circular cylinder were investigated by conducting a POD analysis of the fluctuating surface pressure. At the same time, the effects of the boundary condition of the sidewalls for CFD and the aspect ratio on the fluctuating forces were tested. The following conclusions are based on the results of this study.

The aspect ratio and the boundary condition of sidewalls control the correlation of the fluctuating lift along the axis of the cylinder. Therefore, the cyclic condition should not be used to investigate the correlation

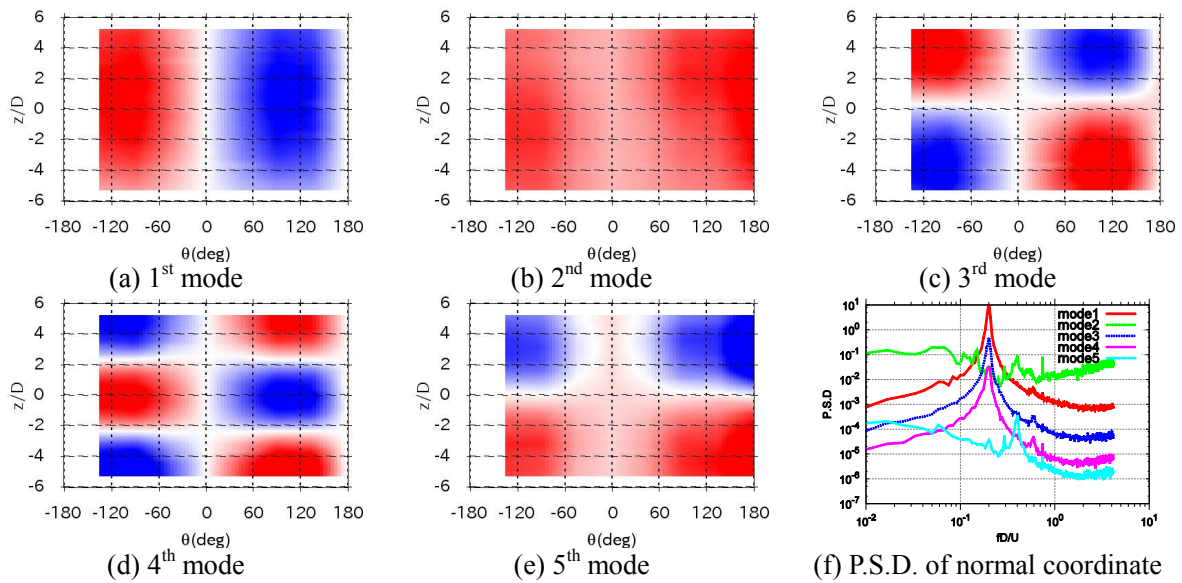


Figure 9: Result of POD analysis for experiment

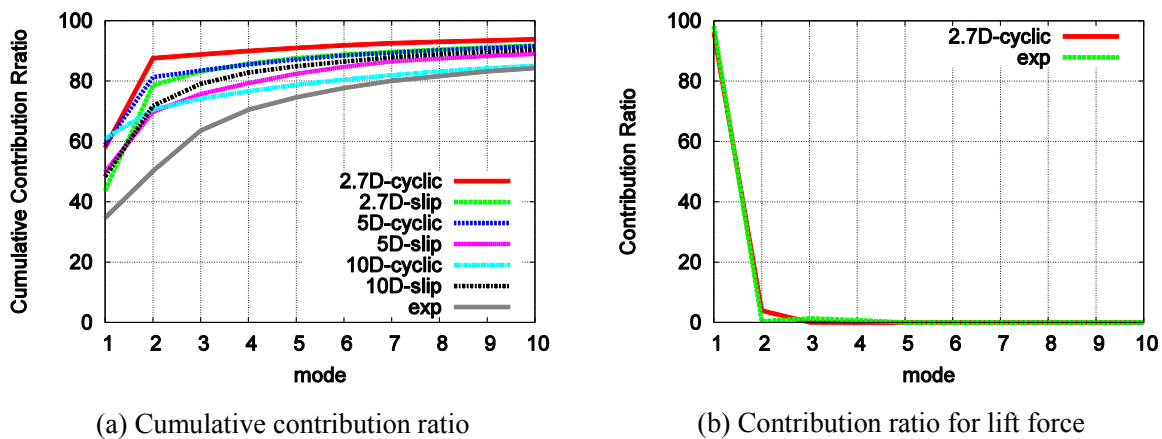


Figure 10: Contribution ratio for results of POD analysis

of the flow along this axis, and it is necessary to ensure an aspect ratio that is as large as possible on CFD in order to reproduce a result close to the natural phenomenon.

The spatial correlation along the cylinder axis of fluctuating forces acting on the cylinder is strengthened by the 1st and 2nd POD modes and weakened by POD modes higher than the 3rd. Moreover, it was found that POD modes beyond the 3rd are controlled by the boundary condition of sidewalls for CFD. Therefore, the cyclic condition should not be used in CFD to investigate the correlation characteristics along the cylinder axis of the flow.

ACKNOWLEDGMENT

This work was supported by JSPS KAKENHI, Grant Number 26420460.

REFERENCES

- 1) Vickery, B. J. : Fluctuating lift and drag on a long cylinder of square cross-section in a smooth and in a turbulent stream, *J. Fluid Mech.*, Vol. 25, Pt. 3, pp. 481-494, 1965.
- 2) El Baroudi, M. Y. : Measurement of two-point correlations of velocity near a circular cylinder shedding a Karman vortex street, UTIA Technical Note, No.31, AFOSR TN-60-835, 1960.
- 3) Keefe, R. T. : An investigation of the fluctuating forces acting on a stationary circular cylinder in a

subsonic stream, and of the associated sound field, Report No.76, Institute of Aerophysics, University of Toronto, 1961.

- 4) OpenFOAM Ltd. : OpenFOAM. <http://www.openfoam.org>, 2011.
- 5) Bienkiewicz, B., Tamura, Y., Ham, H. J., Ueda, H., Hibi, K. : Proper orthogonal decomposition and construction of multi-channel roof pressure, *J. Wind Eng. Ind. Aerodyn.*, Vol. 54-55, pp. 369-381, 1995.